PHYSICAL REVIEW A VOLUME 56, NUMBER 2 AUGUST 1997

# Xenon spectator and diagram $L_3$-$M_{4,5}M_{4,5}$ Auger intensities near the $L_3$ threshold

G. B. Armen,[1] S. H. Southworth,[2] J. C. Levin,[1] U. Arp,[3] T. LeBrun,[2] and M. A. MacDonald[4]
[1]*University of Tennessee, Knoxville, Tennessee 37996*
[2]*Argonne National Laboratory, Argonne, Illinois 60439*
[3]*National Institute of Standards and Technology, Gaithersburg, Maryland 20899*
[4]*Engineering and Physical Sciences Research Council, Daresbury Laboratory, Warrington WA4 4AD, United Kingdom*
(Received 16 May 1997)

Calculations based on the theory of radiationless resonant Raman scattering are employed in the interpretation of new Xe $L_3$-$M_{4,5}M_{4,5}$ Auger spectra recorded using synchrotron radiation tuned to energies *across* the $L_3$ edge. Fits of theoretical line shapes to the spectra are employed in separating intensities due to $nd$ spectator (resonant) and diagram Auger processes. Near-threshold Auger intensity, previously attributed to diagram decay, is found to be due to the large-$n$ spectator lines that result from postcollision-interaction–induced ''recapture'' of threshold photoelectrons to $nd$ orbitals. [S1050-2947(97)51208-X]

PACS number(s): 32.80.Hd, 32.80.Fb, 32.80.Rm

Auger spectra photoexcited by near-threshold radiation show a number of interesting features. Just above threshold, diagram Auger lines are distorted and shifted from their high-energy forms by postcollision interaction (PCI) between the escaping photo- and Auger electrons [1]. Just below threshold, narrow spectator (or resonant) Auger lines are observed, associated with electron excitation to Rydberg orbitals. As threshold is approached from either direction these two regimes are blended. In recent years theoretical understanding of such processes has evolved to the point where the whole can be described within the context of radiationless resonant Raman scattering (RRRS) [2]. Historically, observations of the Xe $L_3$-$M_{4,5}M_{4,5}$ spectrum excited with x rays near the $L_3$ edge have played a major role in the development of our ideas about such threshold behavior: The resonant Raman Auger effect was first identified by Brown *et al.* [3] in such a pioneering study. In subsequent work [4], the process was mapped out in a more quantitative fashion, guided by the first fully quantum mechanical calculations based on the lowest-order scattering-theory formalism of the problem [5]. While this latter work employed theory to interpret subthreshold effects, its focus centered on PCI effects in the region slightly above threshold.

The present work introduces results of new Xe $L_3$-$M_{4,5}M_{4,5}$ data analyzed in light of new RRRS calculations. The data represent a complete set of high-resolution spectra recorded across threshold, with a photon bandpass nearly half the natural $L_3$-hole width. The calculations are the first in which diagram and spectator line shapes and intensities are computed at photon energies down through and below threshold. While there are numerous details to discuss (to be presented elsewhere) the present letter is focused on the relative probabilities for spectator and diagram Auger decay, and how these probabilities change with incident-photon energy *across* threshold. Recent analysis of Ar photoion yields coincident with $K$-$L_{2,3}L_{2,3}$ decay [6] indicate that the diagram Auger probability is suppressed below and near threshold by PCI-induced photoelectron recapture [7] into bound spectator orbitals. The present study of the evolution of inner-shell Auger spectra across threshold provides a more direct investigation of this effect. Our calculations for the Xe $L_3$-$M_{4,5}M_{4,5}$ case show a large suppression of threshold diagram intensity, and fits of the theoretical line shapes to the data are shown to be consistent with this picture. We find that features of the spectrum previously associated predominantly with diagram decay are in fact a composite of large-$n$ spectator lines.

Near the Xe $L_3$ threshold there are two distinct processes that lead to ejection of electrons with kinetic energy *near* the nominal $L_3$-$M_{4,5}M_{4,5}$ Auger energy: In the diagram Auger (double ionization) process, $\mathrm{Xe}+\omega\rightarrow\mathrm{Xe}[2p_{3/2}]xd \rightarrow\mathrm{Xe}[3d^2]+e_p^-+e_A^-$, an Auger electron $e_A^-$ and a slow photoelectron $e_P^-$ are emitted. In the spectator Auger (single ionization) process, $\mathrm{Xe}+\omega\rightarrow\mathrm{Xe}[2p_{3/2}]xd\rightarrow\mathrm{Xe}[3d^2]nd +e_A^-$, the ''photoelectron'' remains bound to the residual ionic core in an $nd$ ''spectator'' orbital. In either case, the amplitude for direct excitation of the final states is weak, and the transitions are mediated by excitations to virtual intermediate states associated with the $L_3$ hole ''followed'' by Auger decay. The amplitudes for traversing all $xd$ (bound or continuum) intermediate states [8] must be summed; coherence between alternate paths affects cross sections [6] and produces PCI distortion of diagram line shapes [9].

The experiment was conducted on NIST X-24A beam line at the National Synchrotron Light Source [10]. X rays, energy selected by a Si (111) double-crystal monochromator, were focused onto a xenon gas jet within the source region of a commercial cylindrical-mirror electron-energy analyzer (CMA) [11]. The chamber background pressure was maintained at $2\times10^{-4}$ torr. For photon-energy calibration the CMA was set to measure low energy ($\approx$40 eV) electrons as the photon energy was scanned across threshold. Emission of these electrons is the result of Auger cascades initiated by $L_3$ ionization, and their yield provides an analog of an absorption edge. The maximum of this $L_3$ ''electron-edge'' was employed as a reference point for defining relative photon energies ($\omega_{\mathrm{rel}}$). While similar in appearance to the $L_3$ absorption edge [12], the maximum of the electron edge need not occur at the same photon energy. In recording the $L_3$-$M_{4,5}M_{4,5}$ spectra at set photon energies, the CMA was operated in the retarding mode with a 50-eV pass energy.

 

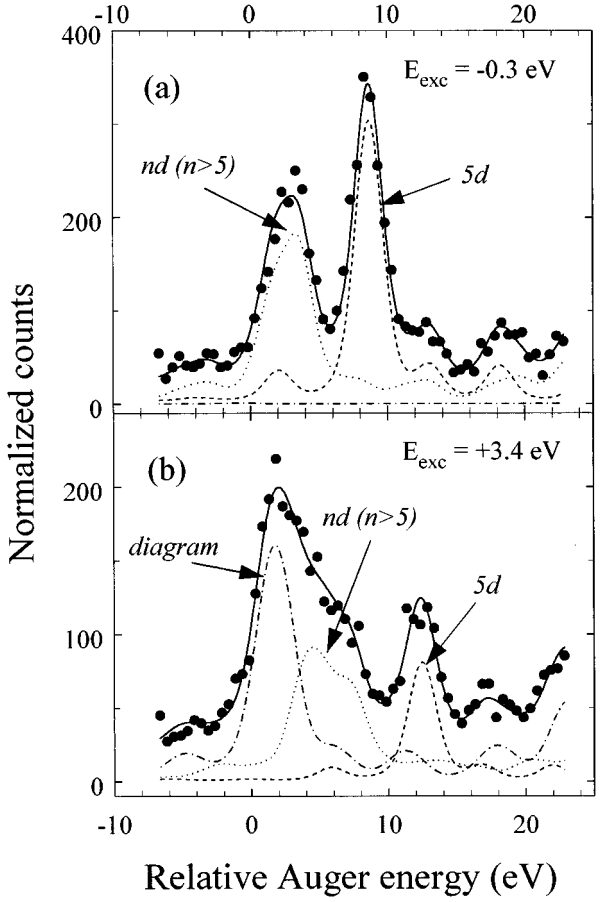


FIG. 1. Xe $L_3$-$M_{4,5}M_{4,5}$ Auger spectra, excited 0.3 eV below (a) and 3.4 eV above (b) the $L_3$ threshold. Theoretical line shapes fitted to the data indicate contributions from $5d$ (dashed line), $nd$ for $n>5$ spectator (dotted), and the diagram (dash-dotted) Auger processes. Electron kinetic energy is plotted relative to the nominal $L_3$-$M_4M_5(^1G_4)$ energy $\varepsilon_A^0$.

Typical auger spectra are displayed in Fig. 1 for photon energies above and just below the $L_3$ threshold ($\approx$4786.3$\pm$0.6 eV [12]). The spectra are complex due to the overlapping contributions from spectator and diagram multiplets. In order to compare experiment with theory, the measured spectra were fit to the functional forms of calculated spectra.

The spectator and diagram cross sections were calculated using the procedure outlined in detail in Ref. [6]: Relaxed, nonrelativistic, Hartree-Fock (HF) wave functions were employed for the xenon ground, intermediate, and final states in the RRRS expression for the $nd$ spectator cross sections ($n=5,...,10$). A quantum-defect-like scaling [6] was employed in deriving intensities and shapes of $n=11,...,\infty$ lines from the $n=10$ calculation. Full relaxation was employed in the calculation of the ground- to intermediate-state excitation amplitudes. The width of the intermediate $L_3$-hole state was taken as $\Gamma_i=2.82$ eV [13]. Cross sections were calculated as a function of excess energy $E_{exc}\equiv\omega-I(L_3)$, the photon energy relative to the $L_3$ threshold. The diagram cross section was derived by subtracting the total spectator cross section from the calculated total Auger cross section [6]. *Natural* spectator line shapes were assumed Lorentzian with widths of 1.0 eV [14] and relative HF energies. Diagram line shapes were approximated using intermediate and final-state continuum functions, which were solutions of the *direct* HF potential only [4,6,9] but agree with full-HF calculations [9] existing in the above-threshold region. The lines were suitably [15] averaged to account for experimental widths: the x-ray bandpass was taken as 1.5 eV and the spectrometer resolution as 1.1 eV, this combination being consistent with estimated values and with observed line widths.

The diagram spectrum consists of a number of multiplet lines dominated by the $M_4M_5(^1G_4)$ line [3]; this line and its spectator analogs are the focus of the current experiment. Well below threshold ($E_{exc}\approx-5$ eV) a single peak is observed corresponding to the $(^1G_4)5d$ spectator final state(s) [3,4] and a ''background'' which is largely due to other *core*-multiplet components [16]. As photon energy is increased, the kinetic energy of the $5d$ line increases and a second peak develops about 5 eV lower in kinetic energy. As threshold is approached, this second peak gains intensity relative to the $5d$ line, and widens. This ''second'' peak arises from the population of $(^1G_4)nd$ $(n>5)$ spectator states, mixed with a previously unknown quantity of the diagram $^1G_4$ line [4]. Above threshold ($E_{exc}>0$) the spectator lines continue to disperse to higher kinetic energies while losing intensity, and eventually a PCI distorted and shifted $^1G_4$ diagram line emerges whose energy tends to the nominal Auger energy, $\varepsilon_A^0=I(L_3)-I(M_4M_5\ ^1G_4)$, at large excitation energies [1,4].

Xenon $L_3$-$M_{4,5}M_{4,5}$ spectra were recorded over a spread of 30 eV in kinetic energy using 0.5 eV steps. Incident x-ray energies ranged from 5 eV below to 15 eV above the $L_3$ threshold. Additionally, several spectra were recorded at larger excess energies from 50 to 200 eV. To compare with theoretical predictions, a least-squares fit of the data to calculated line shape intensity was performed using a limited number of parameters. From such a fit, an ''experimental'' partitioning of the ''second'' peak into spectator $(n>5)$ and diagram intensity was accomplished. We employed a fitting function comprised of three distributions: a $5d$ spectator line, a distribution including *all* higher $nd(n>5)$ spectators, and a diagram line. The distribution shapes and relative energies were calculated for each $E_{exc}$, so a fit to a spectrum employed five parameters: three intensities, a flat background, and an absolute energy adjustment. The $(n>5)$ spectator distribution was a composite of many lines, and relative intensities *within* the $(n>5)$ spectator distribution were fixed by theory, determining the overall line shape for a given photon energy.

Because the location of threshold relative to the ''electron-edge'' reference point is uncertain, the experimental $E_{exc}$ was determined as follows: Fits of large-$E_{exc}$ data to semiclassical diagram PCI line shapes [17] were employed to determine the no-shift limit $\varepsilon_A^0$ (a fitted value $\varepsilon_A^0=3381.67\pm0.06$ on our uncalibrated absolute-energy scale). The *relative* kinetic energy of the maximum of an $nd$ spectator line is given [6] as $\varepsilon_{nd}-\varepsilon_A^0=E_{exc}+i_{nd}^{++}+\delta(E_{exc})$, where $i_{nd}^{++}$ is the binding energy of the $nd$ electron to the double-hole core and $\delta$ is the deviation from linear dispersion due to instrumental averaging [15]. Observed values of $\varepsilon_{5d}$, together with $\varepsilon_A^0$ and calculated values of $i_{5d}^{++}$ and $\delta$ (a

slow function of an assumed $E_{\rm exc}$), were used to find an experimental offset to the relative photon energy; $E_{\rm exc} = \omega_{\rm rel} + E_{\rm offset}$. The result of a least-squares fit was $E_{\rm offset} = 0.51 \pm 0.27$ eV. The error is due to uncertainties in determining $\omega_{\rm rel}$ rather than in fitting the $5d$-peak position (typically $\approx 0.07$ eV). Only the low-$\omega_{\rm rel}$ spectra were employed for this procedure for which the $5d$ line was isolated and prominent. With this offset determined, the excess energy for each data set was defined and employed to calculate the line shapes.

Because a fit must encompass distributions with potentially low intensity, it was found to be crucial to model the ''background'' carefully. To this end, the full $M_{4,5}M_{4,5}$ multiplet structure for the diagram and each spectator Auger process was included in the theoretical line shapes. While in reasonable agreement with intermediate-coupling calculations, the multiplet structure used was taken from fits to $5d$ spectra recorded at $E_{\rm exc} \approx -5$ eV, adjusted to account for the small amount of $6d$ intensity predicted by theory. Also, though of minor importance, a phenomenological $L$-$MMM$ shake-up or -off satellite background from low-resolution extended-scan data was included.

The results of such fits are displayed along with the data in Fig. 1. The solid curve in each panel represents the total fitted line shape. The total is decomposed into component functions: the dashed line is the contribution from the $5d$ spectator multiplet, the dotted line is the $nd(n>5)$ spectator group, and the dashed-dotted line indicates the diagram multiplet. Not shown in the decompositions are the constant backgrounds.

Just below threshold [Fig. 1(a)] the $5d$ line is predominant. The $6d$ and $7d$ lines are the major theoretical components of the $n>5$ spectator group (82% of the total intensity), and their dominance within the group causes the asymmetry of the $n>5$ collective line shape towards higher kinetic energy. Even though excited only 0.3 eV below threshold [$E_{\rm exc} = -0.1\Gamma_i$], the diagram line contributes essentially nothing to the spectrum: a central result of this work.

Just above threshold [$E_{\rm exc} = +3.4$ eV$= +1.2\Gamma_i$, Fig. 1(b)] the $5d$ line has lost intensity relative to the lower-energy peak, which is seen to be a blend of diagram and $nd(n>5)$ spectator lines. Here the $n>5$ distribution is skewed to lower kinetic energies as large-$n$ spectator states are preferentially populated. The diagram line has acquired considerable intensity, but is still narrow due to energy conservation; at larger excess energies it widens and assumes the usual semiclassical PCI line shape with a high-energy flank, and gradually evolves into a symmetric Lorentzian as $E_{\rm exc}$ is increased even further.

The fractional intensity of each line group as a function of $E_{\rm exc}$ can be compared back to theory. Theoretical fractional intensities are obtained from ratios of the relevant partial cross sections to the total, after convolution with the experimental bandpass. The results are displayed in Fig. 2, where agreement between fit results and theory is seen to be quite good. Only the theoretical length-gauge results are indicated in the figure; the velocity and acceleration-gauge *ratios* differ by no more than 0.02. The $5d$ spectator is dominant at low $E_{\rm exc}$, giving way to the higher-$n$ spectators as threshold

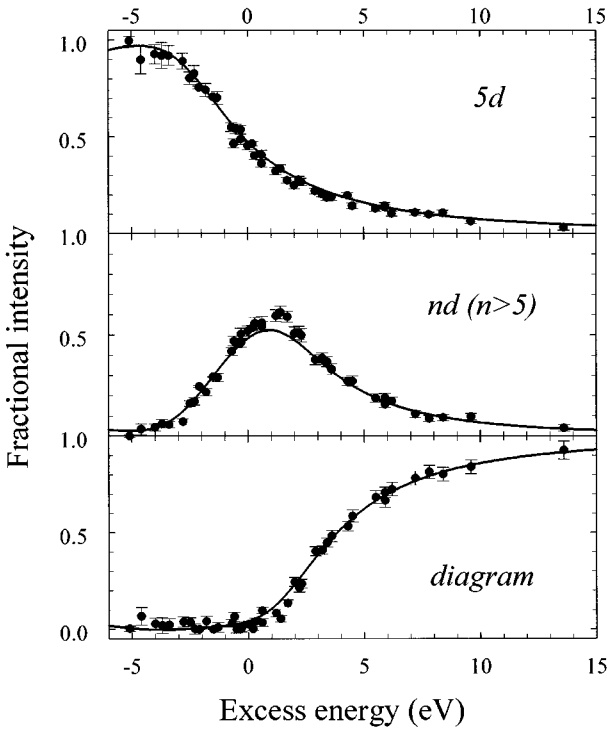


FIG. 2. Results of fitting theoretical line shapes to the data: Plotted are relative intensities (or branching ratios) for each of the line-shape groups outlined in Fig. 1 as a function of incident-photon energy relative to the $L_3$ threshold. The curves indicate the theoretical values, derived from cross-section ratios. The intensity of the diagram process is suppressed until approximately 3.8 eV above threshold.

is approached from below. In simple models of decay, the fractional intensity of the diagram line would be expected to increase from below threshold, with an inflection point at $E_{\rm exc} = 0$ as suggested by the model fit to the photoabsorption spectrum [12]. However, the diagram intensity is seen from Fig. 2 to be delayed until well above threshold: diagram transitions account for only 50% of the emitted intensity 3.8 eV above threshold ($E_{\rm exc} = +1.4\Gamma_i$). Classically, a slowly-escaping photoelectron loses energy when passed by the fast secondary Auger electron due to the sudden change in screening it experiences [1]. This energy loss (the PCI shift, or energy gain of the Auger electron) increases for decreasing photoelectron energy. For photon energies near threshold, the energy loss is so large that the photoelectron must remain bound to the ion, forming a spectator final state. Quantum mechanically, this classical process corresponds to continuum shake-down amplitudes for populating a final spectator state which, in the region above threshold, dominate over the amplitudes for traversing bound intermediate state [6]. It should be noted that this model pertains to atomic or molecular processes. In the solid state, changes in screening can be masked by conduction-band electrons depending on specific characteristics of the material studied (see, e.g., [18,19]).

In conclusion, we have shown that observed Auger spectra evolve with photon energy across threshold in accordance

with theoretical predictions. In particular, the theory indicates a suppression of diagram intensity near and below threshold. However, the good agreement between theory and experiment does not constitute a true experimental partitioning of the spectra into diagram and spectator intensity. Because the diagram line merges continuously into the large -$n$ spectator distribution there is no way, even in principle, to determine such a partition from a noncoincidence experiment alone. What we have shown is a self-consistency between theoretical predictions and the observed Auger profiles. Fit results of the ''second'' peak can only be interpreted in regards to the underlying model used to describe the peak shape. Here we have demonstrated that it is crucial to include large-$n$ spectator satellites in the model. Complementary to Auger spectroscopy, techniques employing ionic charge-state spectroscopy in coincidence with Auger [6] or zero-kinetic-energy electron emission [20] are of interest in pursuing the problem; however, interpretation of such studies also suffer from inherent complications, such as cascade effects. Hence, examining the general problem from as many different vantages as possible is of continued importance.

We thank B. A. Karlin for technical assistance in the experiment. This work is supported by the National Science Foundation and by the U.S. Department of Energy Office of Basic Sciences under Contract No. W-31-109-Eng-38. U.A. is grateful to the Alexander von Humboldt Foundation for financial assistance.

[1] A. Russek and W. Mehlhorn, J. Phys. B **19**, 911 (1986).

[2] T. Åberg and B. Crasemann, in *Resonant Anomalous X-ray Scattering: Theory and Applications*, edited by G. Materlik, C. J. Sparks, and K. Fischer (North-Holland, Amsterdam, 1994), p. 431.

[3] G. S. Brown, M. H. Chen, B. Crasemann, and G. E. Ice, Phys. Rev. Lett. **45**, 1937 (1980).

[4] G. B. Armen, T. Åberg, J. C. Levin, B. Crasemann, M. H. Chen, G. E. Ice, and G. S. Brown, Phys. Rev. Lett. **54**, 1142 (1985).

[5] T. Åberg and G. Howat, in *Corpuscles and Radiation in Matter I*, edited by S. Flügge and W. Mehlhorn, Handbuch der Physick Vol. XXXI (Springer, Berlin, 1982), p. 469.

[6] G. B. Armen, J. C. Levin, and I. A. Sellin, Phys. Rev. A **53**, 772 (1996).

[7] J. Tulkki, T. Åberg, S. B. Whitfield, and B. Crasemann, Phys. Rev. A **41**, 181 (1990).

[8] The $ns$ states are neglected due to their small contribution, calculated to be no more than 4% of the $nd$ intensities (see also Fig. 8, Ref. [12]).

[9] J. Tulkki, G. B. Armen, T. Åberg, B. Crasemann, and M. H. Chen, Z. Phys. D **5**, 241 (1987).

[10] P. L. Cowan, S. Brennan, R. D. Deslattes, A. Henins, T. Jach, and E. G. Kessler, Nucl. Instrum. Methods Phys. Res. A **246**, 154 (1986).

[11] S. H. Southworth, M. A. MacDonald, T. LeBrun, and R. D. Deslattes, Nucl. Instrum. Methods Phys. Res. A **347**, 499 (1994).

[12] M. Breinig, M. H. Chen, G. E. Ice, F. Parente, and B. Crasemann, Phys. Rev. A **22**, 520 (1980).

[13] M. H. Chen, B. Crasemann, and H. Mark, Phys. Rev. A **24**, 177 (1981).

[14] We take $\Gamma[3d^2] \approx 2\Gamma[3d]$, using the results of M. Ohno and R. E. LaVilla, Phys. Rev. A **45**, 4713 (1992).

[15] G. B. Armen and H. Wang, Phys. Rev. A **51**, 1241 (1995).

[16] Additional multiplet splitting due to the spectator electron is negligible (less than 0.1 eV) compared with the resolution and natural width.

[17] M. Yu. Kuchiev and S. A. Sheinerman, Zh. Eksp. Teor. Fiz. **90**, 1680 (1986) [Sov. Phys. JETP **63**, 986 (1986)].

[18] W. Drube, R. Treusch, and G. Materlik, Phys. Rev. Lett. **74**, 42 (1994).

[19] H. Wang, J. C. Woicik, T. Åberg, M. H. Chen, A. H. Gomez, T. Kendelewicz, A. Mäntykenttä, K. E. Miyano, S. Southworth, and B. Crasemann, Phys. Rev. A **50**, 1359 (1994).

[20] T. Hayaishi, E. Murakami, Y. Morioka, E. Shigemasa, A. Yagishita, and F. Koike, J. Phys. B **27**, L115 (1994).